Can. J. Remote Sensing, Vol. 30, No. 2, pp. 137–149, 2004

Inclusion of topographic variables in an unsupervised classification of satellite imagery

Michael A. Wulder, Steven E. Franklin, Joanne C. White, Morgan M. Cranny, and Jeff A. Dechka

Abstract. Unsupervised classification has emerged as a common method for mapping the land cover of large areas with satellite data. Typically, clusters generated by an unsupervised algorithm, such as the K-means, are merged and labelled using a combination of manual and automated methods. Topographic shadows found in areas of high relief, particularly in areas with low sun angles, increase the complexity of land cover classification, as a single land cover class may have very different spectral responses in shadowed and nonshadowed areas of the image. Methods to increase classification accuracies in areas with severe topographic shadows are required for Canadian large area land cover mapping projects. In a standard supervised classification, increases in land cover map classification accuracy have been obtained by including topographic attributes as inputs to the classification algorithm. In this study we investigate the potential of such data as a means to increase the accuracy of an unsupervised land cover classification in a high-relief area in central British Columbia, Canada. Separate datasets were used in cluster labelling and accuracy assessment. Four classification trials were completed: (*i*) using a standard approach without the addition of topographic attributes, (*ii*) using elevation data as an additional input to (*i*), (*iii*) prestratifying the image into shadow and nonshadow areas prior to clustering, and (*iv*) combining the methods used in (*ii*) and (*iii*). The latter provided the highest level of overall attribute accuracy at 80.1%, with a 95% confidence interval of 73.6%–88.6%. This is an improvement over the standard approach, which produced an overall attribute accuracy of 68.7%, with a 95% confidence interval of 59.8%–77.6%. We concluded that the prestratification of an image into areas of shadow and nonshadow prior to clustering in conjunction with the use of elevation data as an input to the clustering process is a practical method to increase classification accuracy in areas of high relief where topographic shadow is problematic.

Résumé. La classification non dirigée est devenue une méthode courante pour la cartographie du couvert à l'aide de données satellitaires dans les régions de grande étendue. Typiquement, des groupements générés par un algorithme non dirigé, comme la méthode des K centroïdes, sont intégrés et étiquetés à l'aide d'une combinaison de méthodes manuelles et automatisées. Les ombres topographiques rencontrées dans les régions de haut relief, en particulier dans les régions caractérisées par de faibles angles solaires, accroissent la complexité de la classification du couvert étant donné qu'une même classe de couvert peut présenter des réponses spectrales très différentes selon qu'on se situe dans des zones ombragées ou non ombragées de l'image. Il est nécessaire de développer des méthodes pour améliorer la précision de classification dans les régions avec des ombres topographiques importantes pour les projets canadiens de cartographie du couvert couvrant de grandes étendues. Dans une classification dirigée conventionnelle, les améliorations de la précision de classification dans le contexte de la cartographie du couvert ont été obtenues grâce à l'ajout à l'algorithme de classification d'attributs topographiques à titre d'intrants. Dans cette étude, nous examinons le potentiel de telles données comme moyen d'accroître la précision d'une classification non dirigée du couvert dans une zone de haut relief dans le centre de la Colombie-britannique, au Canada. Des ensembles de données distincts ont été utilisés pour l'étiquetage des groupements et l'évaluation de la précision. Quatre essais de classification ont été complétés : (*i*) utilisation d'une approche conventionnelle sans l'ajout d'attributs topographiques, (*ii*) utilisation de données d'altitude comme intrant additionnel à (*i*), (*iii*) pré-stratification de l'image en zones ombragées et en zones non ombragées avant le processus de groupement, et (*iv*) combinaison des méthodes utilisées en (*ii*) et (*iii*). Cette dernière a fourni le plus haut taux de précision globale des attributs à 80,1% avec un intervalle de confiance de 95% de 73,6% à 88,6%. Ceci représente une amélioration par rapport à la méthode conventionnelle qui a produit une précision globale des attributs de 68,7% avec un intervalle de confiance de 59,8% à 77,6%. Nous avons conclu que la pré-stratification d'une image en zones ombragées et zones non ombragées avant groupement conjointement avec l'utilisation de données d'altitude à titre d'intrant à la procédure de groupement constitue une méthode pratique pour accroître la précision de classification dans les régions de haut relief où l'ombre topographique est problématique.
[Traduit par la Rédaction]

Introduction

The classification of the land cover of large areas with remotely sensed data is an operational application of satellite image technology (Cihlar, 2000; Franklin and Wulder, 2000). Large regions (Homer et al., 1997), nations (Loveland et al., 1991; Fuller et al., 1994; Cihlar and Beaubien, 1998), continents (Stone et al., 1994), and the entire globe (Loveland

Received 28 July 2003. Accepted 29 October 2003.

M.A. Wulder,[1] J.C. White, M.M. Cranny, and J.A. Dechka. Pacific Forestry Centre, Canadian Forest Service, Natural Resources Canada, 506 West Burnside Road, Victoria, BC V8Z 1M5, Canada.

S.E. Franklin. Department of Geography, University of Saskatchewan, Saskatoon, SK S7N 5A2, Canada.

[1]Corresponding author (e-mail: mike.wulder@nrcan.gc.ca).

and Belward, 1997; Loveland et al., 2000; Hansen et al., 2000) have been mapped with a diverse range of satellite data inputs and spatial resolutions. Unsupervised classification approaches are the most common in these large area land cover classification projects (Franklin and Wulder, 2000).

One robust unsupervised classification method is known as hyperclustering and labelling and involves the generation of many more clusters than expected in the data. The objective of hyperclustering is to ensure that clusters form naturally relative to the spectral information present in the image and are not forced by the restriction to a small number of classes (Swain and Davis, 1978). Following the hyperclustering, a cluster-merging process is developed, which may be manual (supervised) or automated. Once the cluster merging is complete, a labelling process is undertaken. The labelling of classes is at present a manual exercise, requiring an experienced analyst with specific knowledge of the area being mapped and with access to photographic or other spatial data as supporting information. Once all clusters have been labelled, the thematic classified map is complete and an accuracy assessment is undertaken (Czaplewski, 2003). A process of relabelling clusters using additional ancillary information or revisiting common areas of confusion may be implemented until the accuracy of the classification exceeds a user-defined threshold.

Additional ancillary data, which are complementary to the spectral information in the image data and may improve the quality of the maps developed, are required to provide final map accuracies that are acceptable for many applications. For instance, the inclusion of texture (Kushwaha et al., 1994), vegetation indices (Asner et al., 2003), and multitemporal data (Dymond et al., 2002) has been used to increase supervised land cover classification accuracy. In many environments, digital elevation models (DEM) are an obvious choice for use in classification of land cover (Strahler et al., 1978), as discrimination of cover types whose distributions are influenced by variation in elevation is improved with the inclusion of the DEM in the classification (Franklin and Peddle, 1989; Franklin et al., 1994; Franklin et al., 2000a; 2000b). One approach is to use the DEM data, or derivatives such as aspect and slope, as supplemental logical channels in the classification input data (Strahler et al., 1978; Strahler, 1981, Hutchinson, 1982); another is to stratify the image data using the DEM (Skidmore, 1989; Franklin, 1991); another is to modify classifier prior probabilities (Strahler, 1981); and still another is to employ rule-based or expert systems logic (Desachy et al., 1996).

Improved classification accuracies have been reported with the direct incorporation of a DEM into an unsupervised classification approach. Elumnoh and Shrestha (2000) used an ISODATA algorithm with 13 land cover classes in forested highlands and agricultural lowlands in Thailand. Their study site had an elevation range of 15–1671 m. Classification accuracy improved from 65.3% (without the DEM) to 72.4% (with the DEM). The largest improvement was found in discriminating lowland agriculture fields from highland forest classes. Shadow, however, was not a factor in their study area but has been noted by many authors as a major source of classification error in other mountainous regions. For example, Sader et al. (1989) attempted to determine the relationships among tropical forest biomass, successional age classes, and the normalized vegetation index (NDVI). They found that the low sun angle and the resulting cast shadows on steep north- and west-facing slopes reduced the reflectance recorded by the Landsat thematic mapper (TM) sensor and thereby impacted the calculation of the NDVI. They concluded that, as a result of shadow, the methods they developed could not be successfully applied to high-relief tropical forests. Similarly, McGuffie and Henderson-Sellers (1986) recommended that land surface classification for snow budget studies be undertaken with extreme care in high-latitude areas with extreme topographic relief, where low sun angles exacerbate shadow effects. Topographic shadows, combined with other factors, were problematic for snow mapping algorithms using Landsat TM data in their arctic study area.

There are two issues associated with land cover classification in areas of large topographic variability that are relevant to this study: the topographic effect and cast shadows. The topographic effect is defined as the artificial variability in spectral response for a given land cover class, resulting from variations in slope and aspect that is further intensified under conditions of low sun angle and extreme topographic relief (Civco, 1989). When a topographic feature in a mountainous area of high relief blocks direct solar radiation, a cast shadow may result on the adjacent surface, exacerbating the topographic effect. Numerous methods for normalizing the effect of topography, and consequently reducing or removing the impact of shadows, have been presented in the literature (Teillet et al., 1982; Leprieur et al., 1988; Civco, 1989; Colby, 1991; Itten and Meyer, 1993; Meyer et al., 1993); however, methods of topographic normalization cannot be applied to areas of cast topographic shadows because assumptions regarding slope-aspect relationships are violated (Giles, 2001).

In the context of an unsupervised classification process where a nonparametric clustering algorithm is used, there is no need to account for the topographic effect and normalize the spectral response of land cover classes. The existence of topographic shadows (originating from the topographic effect and from adjacent terrain features) will impact the formation of clusters, and it is therefore necessary to account for the presence of shadows, either through prestratification or through the use of additional ancillary inputs to the clustering process that will improve the partition of measurement space (Strahler, 1981).

To meet provincial, national, and international monitoring and reporting needs, the Canadian Forest Service, in partnership with the Canadian Space Agency, is developing a land cover map of the forested area of Canada as a component of the Earth Observation for Sustainable Development of Forests (EOSD) program (Wulder et al., 2003). Canada is a large and geographically diverse country. Stratification of a DEM of Canada with the Landsat Worldwide Referencing

System illustrates, on a scene basis, the degree and spatial distribution of topographic variability (Wulder and Seemann, 2001). Large ranges in elevation characterize much of British Columbia, with 65% of the 75 Landsat scenes covering the province having elevation ranges greater than or equal to 2000 m. These large elevation ranges equate to a number of radiometric and topographic issues and, when coupled with a low sun angle at the time of satellite overpass, create significant shadowing effects in the data. At present, areas of topographic shadow are identified as a separate class within the EOSD classification system, with no effort to further characterize them (Wulder and Nelson, 2001; Wulder et al., 2002). Based on the predominance of areas with high topographic variability in British Columbia, large areas of land may be unaccounted for in the EOSD land cover mapping program. The purpose of this research is to address the problem that topographic shadows pose in an unsupervised land cover classification process (Wulder et al., 2002) and to examine the increase in classification accuracy that can be obtained by including a DEM or its derivatives in an unsupervised cluster and labelling approach for land cover mapping of a predominantly forested, high-elevation area in central British Columbia.

Study area

The study area is located in central British Columbia, Canada, approximately 100 km northeast of Prince George (**Figure 1**). Located in the foothills of the Hart Ranges of the Rocky Mountains, the elevation varies from 660 to 2450 m. The main climax tree species are hybrid white spruce (*Picea glauca* × *engelmannii*) and subalpine fir (*Abies lasiocarpa*). Seral species such as lodgepole pine (*Pinus contorta*) and Douglas fir (*Pseudotsuga menziesii*) are also common in mature forests. Lodgepole pine occupies the drier, nutrient-poor sites, and Douglas fir is less common and requires dry, rich soil. Other common tree species in the area are black spruce (*Picea mariana*), trembling aspen (*Populus tremuloides*), balsam poplar (*Populus balsamifera*), and paper birch (*Betula papyrifera*). The climate of the region is continental and is characterized by cold, snowy winters with short, warm, moist summers. There is moderate precipitation, 440–900 mm each year, with 25%–50% of the precipitation in the form of snow. Forest harvesting is the primary human disturbance activity in this area for dense coniferous forest types.

Image and ancillary data

The Landsat-7 enhanced thematic mapper plus (ETM+) image utilized in this research (path 48, row 22) is centred at 54°17′13.35″N latitude, 121°8′54.70″W longitude and was acquired on 23 September 2000. The imagery was orthorectified in Universal Transverse Mercator (UTM) zone 10 (North American Datum of 1983 (NAD 83)) to a 30 m pixel spacing with a root mean square (RMS) error of less than 0.5 pixels in both *x* and *y* directions. The imagery was calibrated and converted to top-of-atmosphere radiance values following the theory of Markham and Barker (1986) and described in Peddle et al. (2003). The final preprocessing step was the creation of an analysis subset of a 1050 pixels × 1050 pixels (31.5 km × 31.5 km) area.

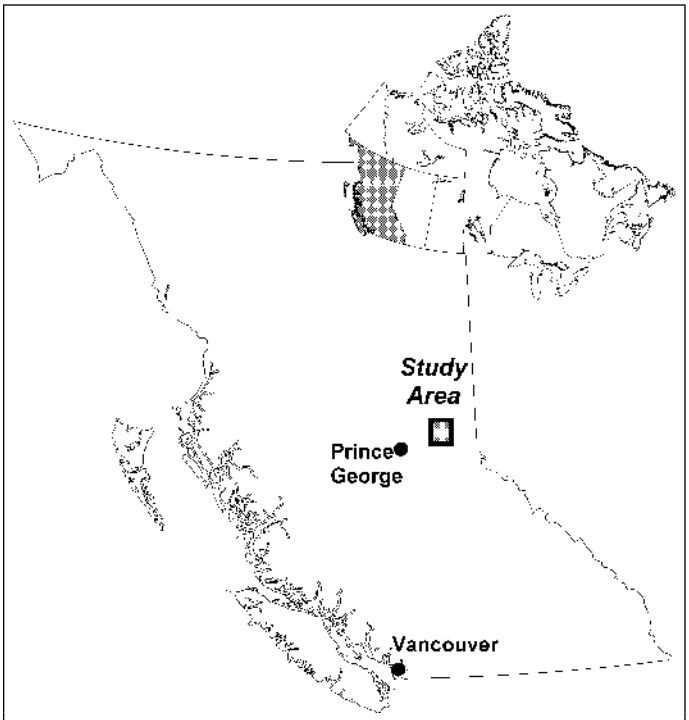

Figure 1. Location of the study area, ~100 km northeast of Prince George, British Columbia, Canada. The 31.5 km × 31.5 km study region is centred at 54°17′13.35″N, 121°8′54.70″W.

The Base Mapping and Geomatics Services Branch (1996) supplied the gridded DEM product. The grid spacing is 25 m and the DEM was created from the 1:20 000 scale Terrain Resource Information Management (TRIM) DEM. The DEM was resampled to correspond to the 30 m image spatial resolution. Aspect and slope (in degrees) were derived from this DEM using standard methods. These data were scaled to the same numerical range as that of the imagery (0–255) to ensure that all input channels had equal weighting in the clustering procedure (Strahler, 1981). The importance of scaling these data prior to inputting them into the K-means clustering algorithm is essential and is often not reported in the methodologies of studies that incorporate these data for the purpose of improving discrimination between land cover classes. The K-means clustering algorithm is designed to minimize cluster variability, and cluster variability is measured with respect to the mean values of the classifying variables. If multiple variables are used to define the clusters, the dissimilarities between the clusters are measured in multidimensional space using Euclidean distance (Tou and Gonzalez, 1974). A higher variance in one input variable will force the clusters to be partitioned more discretely in that dimension of measurement space than in the dimensions

corresponding to the other inputs (Strahler, 1981). **Figures 2A** and **2B** illustrate the effect that including the unscaled elevation data has on the formation of the clusters in two different subregions of the study area. Inputs to the clustering in this example included the six optical Landsat channels and an intrapixel variance channel, all having a digital number range of 0–255, and the unscaled elevation channel, which has a range of 650–2500. The higher variance in the unscaled elevation data is clearly dominating the clustering process. **Figures 2C** and **2D** show the same areas clustered with the elevation data scaled to the same range and the image and intrapixel variance channels (0–255). As a result of this effect,

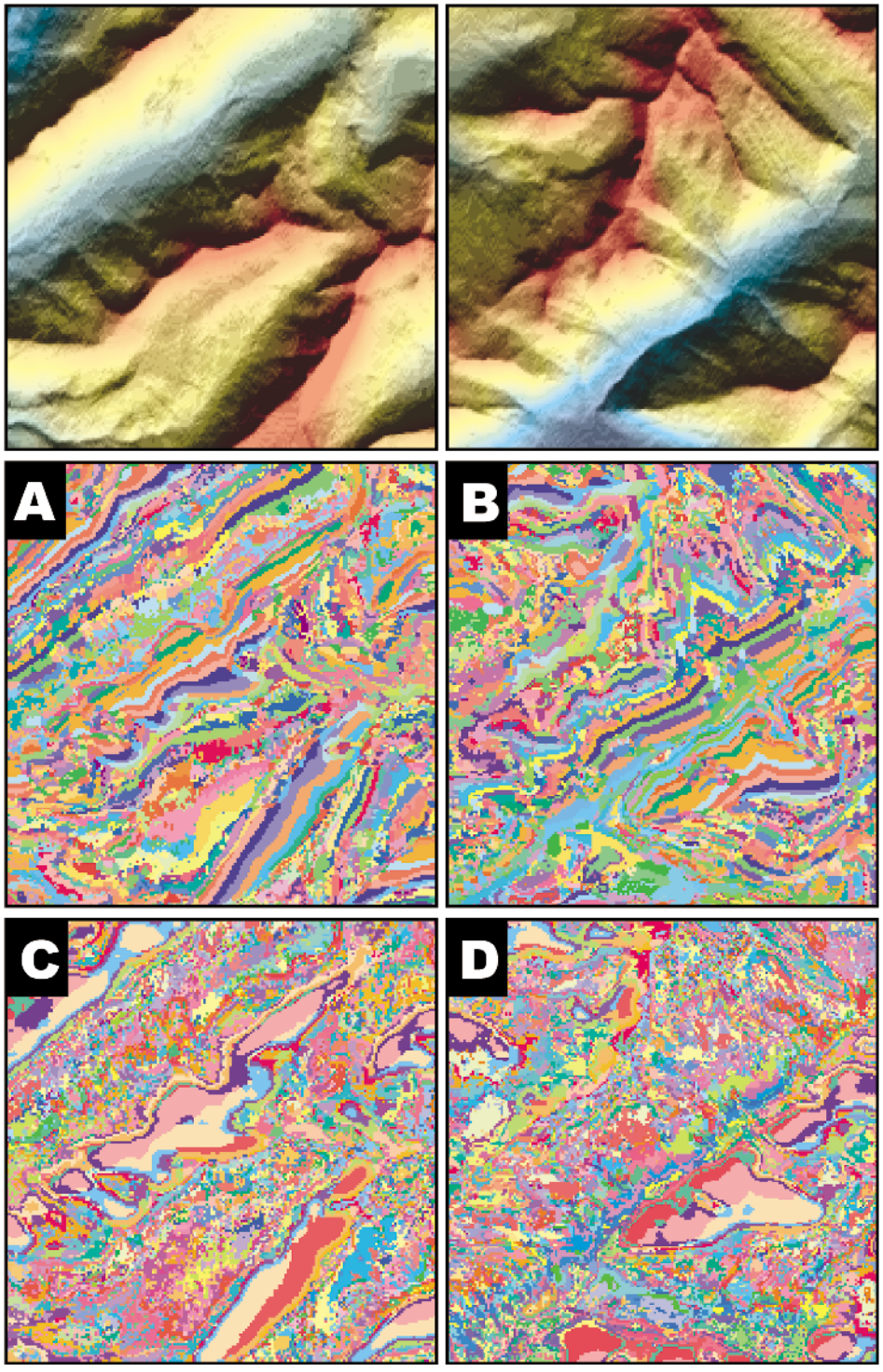

Figure 2. Differences in output K-means cluster shape when the DEM is not scaled to the same range as that of the image data (A and B) and when the DEM is scaled to the same range as that of the image data (C and D).

all of the topographic variables used in this study were scaled to the same range as that of the image data.

The reference data used for the accuracy assessment were generated from the provincial forest inventory data and are current to 1999 conditions. There was no additional forest harvesting between the date of the last forest inventory update in 1999 and the Landsat ETM+ image acquisition date in September 2000. The forest inventory attributes were used as a proxy for the EOSD classification, and classes were constructed using the EOSD membership rules. The forest inventory data were collected from 1:15 000 scale air photographs and are considered a reliable source of validation for the classified image products.

Methods

Preliminary analysis indicated that the majority of land cover classes within the study area were not normally distributed for elevation, aspect, and slope, primarily because of the predominance of topographic shadow in the image and the broad spectral nature of the classes. Logistic regression models verified that land cover classes did not vary systematically with elevation, aspect, and slope, when considered singularly and in all possible combinations (Strahler, 1981). Thus, there was no evidence to suggest that a model that incorporated any or all three topographic features into the clustering process would directly result in a more accurate classification.

Based on this analysis, effort was focused on alleviating the impact of shadow rather than attempting to build a model around nonexistent relationships between the classes of interest and topographic variables. A strategy for addressing the problem of shadow in the Landsat-7 ETM+ image resulted in the completion of four classification trials as outlined in **Table 1**. The initial classification trial was the control and was conducted using the current methodology implemented by the EOSD land cover mapping program, as outlined in Wulder et al. (2002). This classification procedure involves prestratifying each image into four broad categories based on an NDVI. Each stratum is then processed separately using a K-means clustering algorithm. The input variables for the classification included the six Landsat ETM+ optical bands and one texture measure. The intrapixel texture measure is computed from a 3 × 3 variance of the 15 m resolution panchromatic ETM+ channel (Wulder et al., 2002). The intrapixel texture is resampled to match the 30 m spatial resolution of the optical channels prior to inclusion in the clustering algorithm. Based on these inputs, a hyperclustering approach was used to generate a maximum of 241 initial clusters. These clusters were then aggregated to seven of the 21 broad land cover classes relevant to the area (Wulder and Nelson, 2001) using ancillary data (e.g., provincial vegetation inventory maps developed from air photograph interpretation and field visits). The list of land cover classes included rock, water, tall shrub, low shrub, coniferous open, coniferous sparse, and mixedwood open. The only deviation from this methodology was in the manner with which shadows were classified. Rather than assigning classes to shadows, attempts were made to assign clusters found in these areas to relevant land cover classes.

The methods used in the second trial were identical to those in the first trial; however, the scaled elevation data were added as input to the clustering process. For the third classification trial, the solar incidence angle was calculated for each pixel in the image and subsequently used to identify areas of shadow and nonshadow. The NDVI strata generated as part of the standard methodology were further partitioned into areas of shadow and nonshadow, resulting in eight distinct strata that were each clustered separately. The solar incidence angle is the angle that a ray of solar radiation makes with a line perpendicular to the surface and is a function of both solar direction and local topography. For example, a horizontal

Table 1. Inputs and methods for classification trials.

Classification trial	Inputs	Methods
(1) Standard EOSD clustering methodology	Six Landsat ETM+ optical channels and one intrapixel texture channel (see Wulder et al., 2002)	Image is stratified using four separate masks generated from an NDVI (per Wulder et al., 2002); clustering is done separately on each stratum
(2) Inclusion of elevation data as an input	Six Landsat ETM+ optical channels and one intrapixel texture channel (per Wulder et al., 2002) and elevation (scaled)	Image is stratified using four separate masks generated from an NDVI (per Wulder et al., 2002); clustering is done separately on each stratum
(3) Prestratification of imagery into shadowed and unshadowed	Six Landsat ETM+ optical channels and one intrapixel texture channel (per Wulder et al., 2002)	Image is stratified using four separate masks generated from an NDVI (per Wulder et al., 2002); these strata are subsequently divided into areas of shadow and nonshadow, resulting in eight strata to which clustering is applied separately
(4) Prestratification of imagery into shadowed and unshadowed *and* the inclusion of elevation data as an input	Six Landsat ETM+ optical channels and one intrapixel texture channel (per Wulder et al., 2002) and elevation (scaled)	This method combines trials 2 and 3; image is stratified using four separate masks generated from an NDVI (per Wulder et al., 2002); these strata are subsequently divided into areas of shadow and nonshadow, resulting in eight strata to which clustering is applied separately

surface that is parallel to the sun would have a solar incidence angle of 90°. Solar incidence angle is calculated using the solar azimuth angle, the elevation angle of the sun, and the distance to the sun at the time of image acquisition (Lillesand and Keifer, 1987). These variables, exclusive of distance to the sun, are recorded at the time of image acquisition as a component of image meta-data. **Figure 3** illustrates that for this study area, incident angles less than 34° were selected to delimit areas of shadow, based on interactive viewing of areas of the image with steep terrain as per Strahler (1981). The appropriate solar incidence values that will discriminate shadow in an image will vary according to (*i*) the date of image acquisition and the location of the study area (related to varying solar azimuth and elevation angles), and (*ii*) the nature and orientation of the local topography.

The fourth classification trial combined the methods used in the second and third trials: the image was stratified into areas of shadow and nonshadow, and elevation data were used as one of the inputs to the clustering process. At the completion of the labelling process, each result was assessed for accuracy based on a separate set of randomly selected validation data. A stratified sample design, as described by Czaplewski (2003), was adopted and 15 samples in each of the seven class strata were randomly selected from the polygon centroids of the existing forest inventory of the study area in which proxy EOSD land cover class labels had been generated using the forest inventory attributes. It was determined that a sample size of 105 would provide confidence thresholds of approximately 72.1% and 93.5% around a desired level of accuracy of 85% (at the 95% confidence level) (Czaplewski, 2003). The sample size of 105 is therefore sufficient for estimating the overall accuracy with confidence and for measuring the relative success of individual classification iterations at achieving the desired target level of accuracy. The error matrices and associated accuracy measures are presented in **Tables 2–5**. The accuracy measures were calculated using joint probabilities to ensure unbiased estimates (Czaplewski, 2003).

Results and discussion

The EOSD land cover mapping project is focused on mapping the forested area of Canada. The dominant forest classes found within this study area are open coniferous and sparse coniferous, occupying 54% and 12% of the study area, respectively. The other dominant class in the image is rock (31%). The estimated overall accuracies are summarized in **Table 6**. **Figure 4A** shows an enhanced red–green–blue (RGB) composite of the study image, and **Figure 4B** is calculated solar

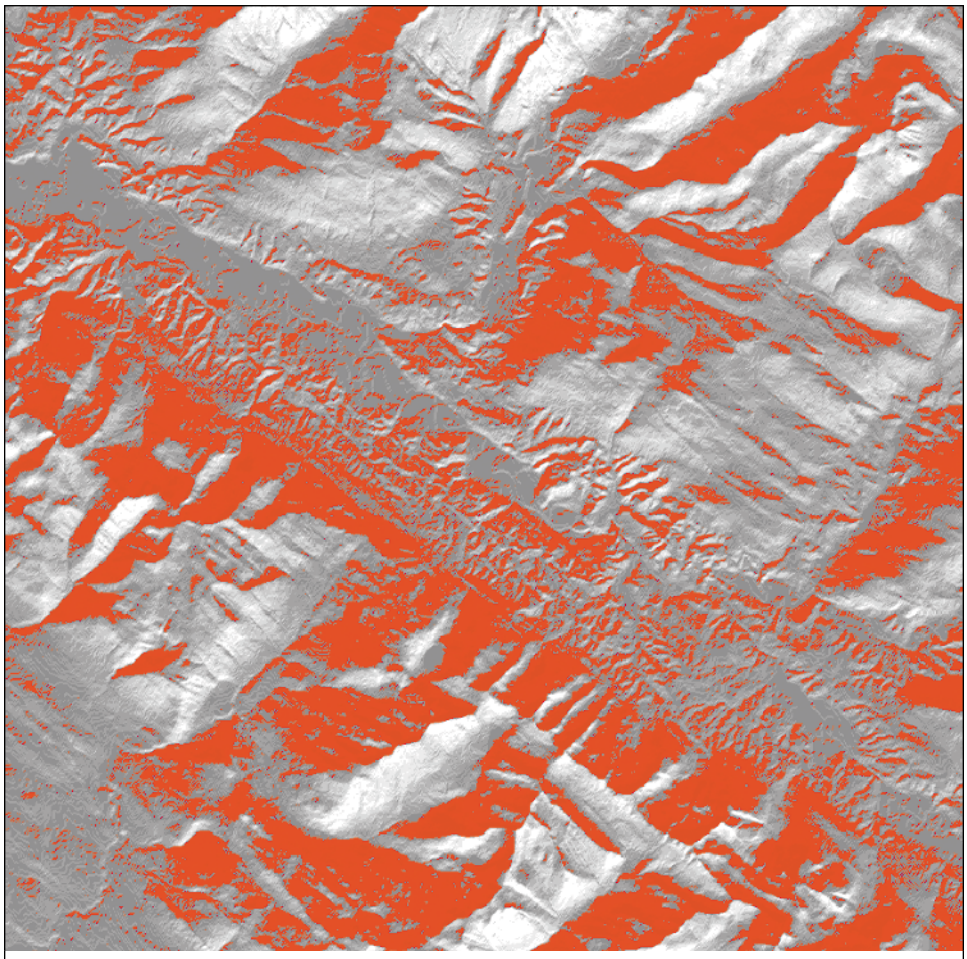

Figure 3. Calculated solar incidence angle, with angles less than 34° shown in red.

Table 2. Error matrices and associated accuracy measures for the unsupervised classification using standard methods with no additional topographic attributes.

(A) Count of points from stratified sample

	Classified image							
Reference	4	6	7	8	15	16	21	Total
4	**12**	0	0	1	0	2	0	15
6	10	**0**	1	0	2	0	2	15
7	6	0	**0**	0	5	4	0	15
8	6	0	1	**2**	5	1	0	15
15	1	0	0	0	**11**	3	0	15
16	2	0	0	0	6	**6**	1	15
21	4	0	0	0	8	1	**2**	15
Total	45	6	9	11	52	33	26	105

(B) Estimates (%) from stratified sample

	Classified image							
Reference	4	6	7	8	15	16	21	Total
4	**24.5**	0.0	0.0	2.0	0.0	4.1	0.0	30.6
6	0.8	**0.0**	0.1	0.0	0.2	0.0	0.2	1.2
7	0.7	0.0	**0.0**	0.0	0.6	0.5	0.0	1.8
8	0.2	0.0	0.0	**0.1**	0.2	0.0	0.0	0.5
15	3.6	0.0	0.0	0.0	**39.4**	10.7	0.0	53.7
16	1.6	0.0	0.0	0.0	4.7	**4.7**	0.8	11.8
21	0.1	0.0	0.0	0.0	0.3	0.0	**0.1**	0.5
Total	31.4	0.0	0.1	2.1	45.3	20.1	1.0	100.0

(C) Accuracy measures

	Classified image							
	4	6	7	8	15	16	21	Overall[a]
Estimated user accuracy (%)	77.9	na	0.0	3.2	87.0	23.5	6.2	68.7 (59.8–77.6)
Estimated errors of commission (%)	22.1	na	100.0	96.8	13.0	76.5	93.8	
Estimated producer accuracy (%)	80.0	0.0	0.0	13.3	73.3	40.0	13.3	
Estimated errors of omission (%)	20.0	100.0	100.0	86.7	26.7	60.0	86.7	
Reference area (ha)	29 319	1105	1705	492	51 422	11 327	450	
Estimated area (ha)	30 129	0	106	2020	43 360	19 242	962	

Note: Image classes are as follows: 4, rock; 6, water; 7, tall shrub; 8, low shrub; 15, open coniferous; 16, sparse coniferous; 21, open mixedwood. na, not applicable.

[a]Estimated overall accuracy and 95% confidence interval.

incidence draped over the DEM. **Figures 4C–4G** show examples of the output from each of the four classification trials in a subarea of the full scene.

Using the standard methodology in the first classification trial resulted in an overall classification accuracy of 68.7% for the seven target classes, with a 95% confidence interval of 59.8%–77.6%. The second classification trial, which added scaled elevation data as an input to the K-means clustering, resulted in an overall accuracy of 69.9%, with a 95% confidence interval of 61.2%–78.7%. The use of elevation data in the second trial produced superior results for the open coniferous class, with 80% of this class being mapped correctly on the image compared with 73% in the first trial. The second trial estimates the true area of open coniferous from the sample data to be 51 264 ha, which is only 158 ha more than the actual area of open coniferous identified in the forest inventory. This compares with an estimated area for open coniferous in the first classification of 43 360 ha. The errors of commission for open coniferous were greater in the second trial as a result of increased confusion with rock. **Figures 4D** and **4E** illustrate how the elevation has had a beneficial effect in reducing the variability in the clusters of the first trial and producing a more homogeneous result. In addition, elevation provided a splitting point for cluster "rings" present in the initial classification trial and that resulted in the open coniferous class being located in

Table 3. Error matrices and associated accuracy measures for the unsupervised classification using the elevation data as an additional input to the K-means clustering algorithm.

(A) Count of points from stratified sample

	Classified image							
Reference	4	6	7	8	15	16	21	Total
4	**11**	0	0	0	2	2	0	15
6	0	**4**	2	0	6	1	2	15
7	3	0	**1**	0	8	1	2	15
8	6	0	0	**3**	2	4	0	15
15	0	0	0	0	**12**	2	1	15
16	0	0	1	3	6	**5**	0	15
21	0	0	0	0	9	2	**4**	15
Total	24	10	11	14	60	33	30	105

(B) Estimates (%) from stratified sample

	Classified image							
Reference	4	6	7	8	15	16	21	Total
4	**22.4**	0.0	0.0	0.0	4.1	4.1	0.0	30.6
6	0.0	**0.3**	0.2	0.0	0.5	0.1	0.2	1.2
7	0.4	0.0	**0.1**	0.0	0.9	0.1	0.2	1.8
8	0.2	0.0	0.0	**0.1**	0.1	0.1	0.0	0.5
15	0.0	0.0	0.0	0.0	**42.9**	7.2	3.6	53.7
16	0.0	0.0	0.8	2.4	4.7	**3.9**	0.0	11.8
21	0.0	0.0	0.0	0.0	0.3	0.1	**0.1**	0.5
Total	23.0	0.3	1.1	2.5	53.5	15.6	4.1	100.0

(C) Accuracy measures

	Classified image							
	4	6	7	8	15	16	21	Overall[a]
Estimated user accuracy (%)	97.6	100.0	11.2	4.2	80.2	25.3	3.1	69.9 (61.2–78.7)
Estimated errors of commission (%)	2.4	0.0	88.8	95.8	19.8	74.7	96.9	
Estimated producer accuracy (%)	73.3	26.7	6.7	20.0	80.0	33.3	26.6	
Estimated errors of omission (%)	26.7	73.3	93.3	80.0	20.0	66.7	73.3	
Reference area (ha)	29 319	1105	1705	492	51 422	11 327	450	
Estimated area (ha)	22 039	295	1016	2364	51 264	14 920	3923	

Note: Image classes as in Table 2.
[a]Estimated overall accuracy and 95% confidence interval.

extremely high elevation areas dominated by rock and related features.

For the third classification trial, the image was prestratified into areas of shadow and nonshadow prior to clustering. Shadowed areas accounted for 33% of the total study area. This trial had an overall accuracy of 75.6%, with a 95% confidence interval of 67.4%–83.8%. **Figure 4F** indicates that, although the stratification of the image into areas of shadow and nonshadow has improved overall accuracy, the classified output in this area suggests there is minimal visual difference between this trial and the first trial. The open coniferous class is mapped with 93% accuracy in this trial, and the area for this class is estimated at 59 276 ha. The increase in accuracy for this one class has resulted in the increase in overall accuracy from the initial trial. The other dominant class by area is rock, and in this classification 73.3% of the rock in the study area is classified correctly on the image. **Figure 4F** illustrates the aforementioned cluster rings of open forest that were problematic in the first classification trial. In an attempt to overcome this problem, elevation was incorporated into the method used for this trial as the fourth and final classification trial.

The final classification trial, which included stratification of shadowed and nonshadowed areas and used elevation as input, provided an overall classification accuracy of 81.1%, with a 95% confidence interval of 73.6%–88.6%. This classification produced the most consistent estimates of accuracy across all classes, as indicated by the reporting of accuracy measures and

Table 4. Error matrices and associated accuracy measures for unsupervised classification using solar incidence angle to stratify image into areas of shadow and nonshadow.

(A) Count of points from stratified sample

	Classified image							
Reference	4	6	7	8	15	16	21	Total
4	**11**	0	0	1	2	1	0	15
6	5	**6**	0	0	2	0	2	15
7	6	0	**0**	0	8	0	1	15
8	6	0	0	**3**	2	4	0	15
15	1	0	0	0	**14**	0	0	15
16	4	0	0	0	8	**3**	0	15
21	2	0	0	0	7	1	**5**	15
Total	39	12	7	12	58	25	29	105

(B) Estimates (%) from stratified sample

	Classified image							
Reference	4	6	7	8	15	16	21	Total
4	**22.4**	0.0	0.0	2.0	4.1	2.0	0.0	30.6
6	0.4	**0.5**	0.0	0.0	0.2	0.0	0.2	1.2
7	0.7	0.0	**0.0**	0.0	0.9	0.0	0.1	1.8
8	0.2	0.0	0.0	**0.1**	0.1	0.1	0.0	0.5
15	3.6	0.0	0.0	0.0	**50.1**	0.0	0.0	53.7
16	3.2	0.0	0.0	0.0	6.3	**2.4**	0.0	11.8
21	0.1	0.0	0.0	0.0	0.2	0.0	**0.2**	0.5
Total	30.5	0.5	0.0	2.1	61.9	4.6	0.4	100.0

(C) Accuracy measures

	Classified image							
	4	6	7	8	15	16	21	Overall[a]
Estimated user accuracy (%)	73.5	100.0	na	4.8	81.0	51.7	36.5	75.6 (67.4–83.8)
Estimated errors of commission (%)	26.5	0.0	na	95.2	19.0	48.3	63.5	
Estimated producer accuracy (%)	73.3	40.0	0.0	20.0	93.3	20.0	33.3	
Estimated errors of omission (%)	26.7	60.0	100.0	80.0	6.7	80.0	66.7	
Reference area (ha)	29 319	1105	1705	492	51 422	11 327	450	
Estimated area (ha)	29 256	442	0	2053	59 276	4 381	411	

Note: Image classes as in Table 2. na, not applicable.
[a]Estimated overall accuracy and 95% confidence interval.

estimated areas in **Table 5**. The trial resulted in 87% of open coniferous, 60% of sparse coniferous, and 87% of rock being mapped correctly. This classification also produced the highest level of accuracy for the water class at 53.3%. As was the case for the second classification trial, the elevation data provided a valuable splitting point for clusters and prevented the occurrence of open and sparse coniferous classes in extremely high elevation areas where they are not likely to be found.

Omission errors were greater than 65% for tall shrub, low shrub, and open mixedwood classes and greater than 50% for the water class in all of the classification trials. These were very rare classes in the image, with each representing 1% or less of the total study area. In addition, the water features in the study area have unique characteristics that contribute to the low accuracy for this class. There are 1104 ha of water in the study area, 234 ha of which are small lakes with an average size of 2 ha; 16 ha of these small lakes were located in areas of topographic shadow. River segments represented 870 ha, with an average size of 20 ha. These segments were long, narrow, and sinuous, with 74 ha of these river segments located in areas of topographic shadow. Given the unique characteristics of the water features in this image, it is not surprising that classification accuracies for water are very low. Commission errors were high for the sparse coniferous class in all trials, primarily resulting from confusion with the open coniferous class, suggesting that within this study area these two classes may be difficult to separate spectrally.

Table 5. Error matrices and associated accuracy measures for unsupervised classification using solar incidence to stratify the image into areas of shadow and nonshadow and using elevation as input to the K-means clustering algorithm.

(A) Count of points from stratified sample

	Classified image							
Reference	4	6	7	8	15	16	21	Total
4	**13**	0	0	0	1	1	0	15
6	0	**7**	2	0	2	2	2	15
7	3	0	**2**	0	8	2	0	15
8	4	0	1	**1**	2	7	0	15
15	2	0	0	0	**12**	1	0	15
16	0	0	0	0	6	**9**	0	15
21	0	1	0	0	8	2	**4**	15
Total	26	14	12	9	54	40	27	105

(B) Estimates (%) from stratified sample

	Classified image							
Reference	4	6	7	8	15	16	21	Total
4	**26.5**	0.0	0.0	0.0	2.0	2.0	0.0	30.6
6	0.0	**0.5**	0.2	0.0	0.2	0.2	0.2	1.2
7	0.4	0.0	**0.2**	0.0	0.9	0.2	0.0	1.8
8	0.1	0.0	0.0	**0.0**	0.1	0.2	0.0	0.5
15	3.6	0.0	0.0	0.0	**46.5**	3.6	0.0	53.7
16	0.0	0.0	0.0	0.0	4.7	**7.1**	0.0	11.8
21	0.0	0.0	0.0	0.0	0.3	0.1	**0.1**	0.5
Total	30.6	0.6	0.4	0.0	54.7	13.4	0.3	100.0

(C) Accuracy measures

	Classified image							
	4	6	7	8	15	16	21	Overall[a]
Estimated user accuracy (%)	86.7	94.5	55.8	100.0	85.0	52.9	44.9	81.1 (73.6–88.6)
Estimated errors of commission (%)	13.3	5.5	44.2	0.0	15.0	47.1	55.1	
Estimated producer accuracy (%)	86.7	46.7	13.3	6.7	86.7	60.0	26.7	
Estimated errors of omission (%)	13.3	53.3	86.7	93.3	13.3	40.0	73.3	
Reference area (ha)	29 319	1105	1705	492	51 422	11 327	450	
Estimated area (ha)	29 310	546	407	33	52 413	12 843	267	

Note: Image classes as in Table 2.
[a]Estimated overall accuracy and 95% confidence interval.

Table 6. Summary of estimates of overall accuracy and confidence intervals.

Classification trial	Estimated overall accuracy (%)	Confidence intervals (%)	
		Lower	Upper
1	68.7	59.8	77.6
2	69.9	61.2	78.7
3	75.6	67.4	83.8
4	81.1	73.6	88.3

Conclusions

The combination of solar incidence angle to stratify the image into shadowed and nonshadowed areas and the use of elevation data as an input to the K-means clustering process increased the overall accuracy of land cover classification in our predominantly forested, high-elevation study area of British Columbia, Canada. This classification process is simple to implement, yet provides an increase in accuracy relative to the standard method where no topographic variables are included and does not require the user to expend resources performing complex topographic normalizations or attempting to determine the relationships between land cover classes and various terrain attributes. However, stratification by shadow is

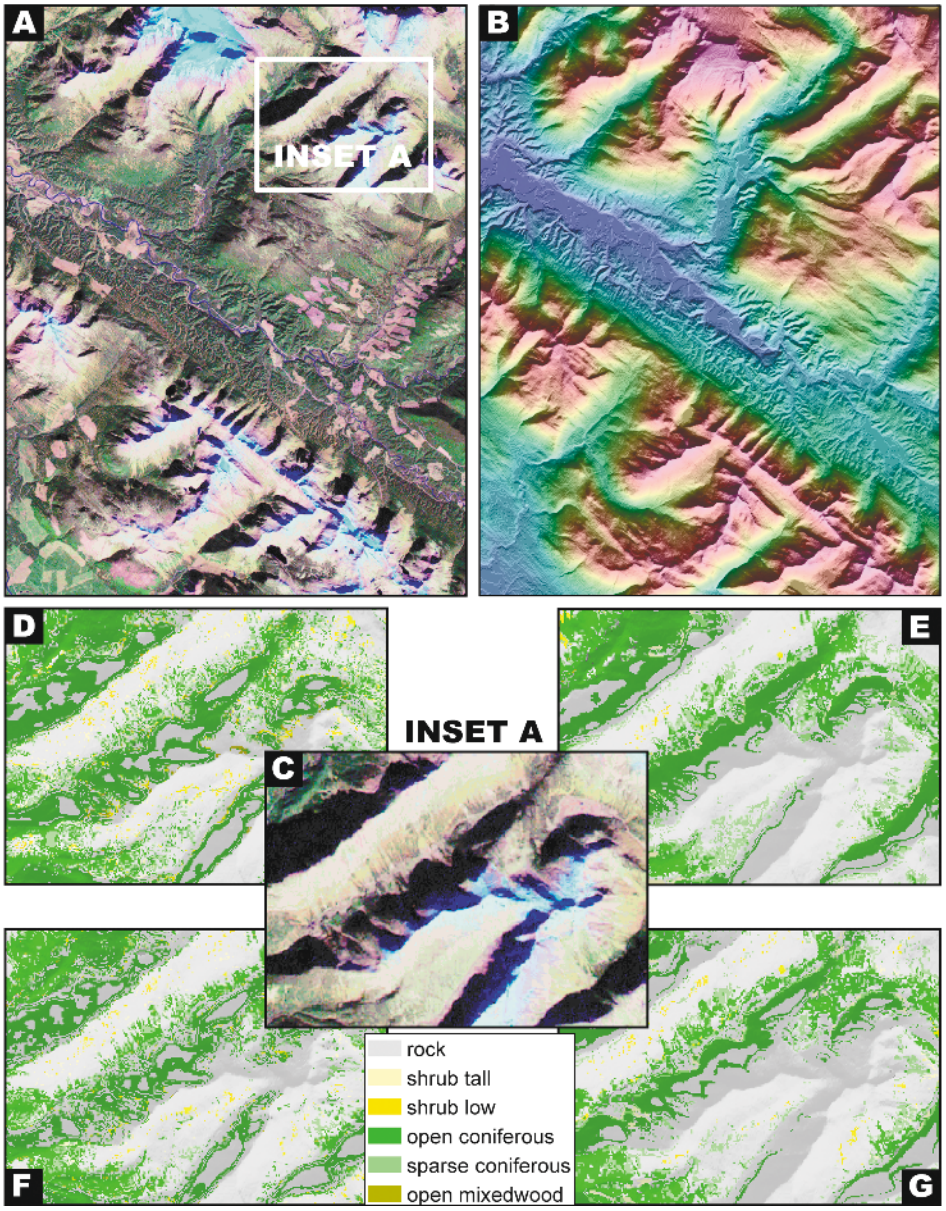

Figure 4. (A) Red–green–blue (RGB) composite of the study area. (B) Calculated solar incidence angle draped over gridded DEM. (C) Enlarged inset from (A). (D) Classification using standard methods. (E) Classification using elevation as input. (F) Classification using solar incidence angle to prestratify image into areas of shadow and nonshadow. (G) Classification combining methods in (E) and (F).

only operationally feasible for those land cover classification products that are created by processing individual scenes (as opposed to mosaicking several scenes together and then classifying them). The methods used could be integrated into the existing EOSD classification methodology with minimal effort for those high-relief areas where topographic shadows are problematic and offer the potential to extract additional land cover information from areas that would otherwise be classed only as shadow. Further trials of this methodology are recommended in areas with (*i*) greater variation in relief, (*ii*) more equitable distributions of land cover classes, and (*iii*) different sun angles and on Landsat imagery collected on different dates.

Acknowledgements

David Seemann of the Canadian Forest Service is thanked for assistance with the data analysis and presentation of results. The Canadian Space Plan of the Canadian Space Agency is acknowledged for funding of Earth Observation for Sustainable Development of Forests (EOSD) (http://www.pfc.forestry.ca/eosd) and this research.

References

Asner, G.P., Hicke, J.A., and Lobell, D.B. 2003. Per-pixel analysis of forest structure: vegetation indices, spectral mixture analysis and canopy reflectance modeling. In *Remote sensing of forest environments: concepts and case studies.* Edited by M. Wulder and S. Franklin. Kluwer Academic Publishers, Dordrecht, The Netherlands. pp. 209–254.

Base Mapping and Geomatics Services Branch. 1996. *Gridded DEM specification, release 1.1*. Base Mapping and Geomatics Services Branch, British Columbia Ministry of Sustainable Resource Management, Victoria, B.C.

Cihlar, J. 2000. Land cover mapping of large areas from satellites: status and research priorities. *International Journal of Remote Sensing*, Vol. 21, No. 6–7, pp. 1093–1114.

Cihlar, J., and Beaubien, J. 1998. *Land cover of Canada, version 1.1, special NBIOME Project*. Canada Centre for Remote Sensing and the Canadian Forest Service, Ottawa, Ont.

Civco, D.L. 1989. Topographic normalization of Landsat Thematic Mapper digital imagery. *Photogrammetric Engineering & Remote Sensing*, Vol. 55, No. 9, pp. 1303–1309.

Colby, J.D. 1991. Topographic normalization in rugged terrain. *Photogrammetric Engineering & Remote Sensing*, Vol. 57, No. 5, pp. 531–537.

Czaplewski, R.L. 2003. Accuracy assessment of maps of forest condition: statistical design and methodological considerations. In *Remote sensing of forest environments: concepts and case studies*. Edited by M. Wulder and S. Franklin. Kluwer Academic Publishers, Dordrecht, The Netherlands. pp. 115–140.

Desachy, J., Roux, L., and Zahzah, E. 1996. Numeric and symbolic data fusion: a soft computing approach to remote sensing image analysis. *Pattern Recognition Letters*, Vol. 17, No. 13, pp. 1361–1378.

Dymond, C.C., Mladenoff, D.J., and Radeloff, V.C. 2002. Phenological differences in Tasseled Cap indices improve deciduous forest classification. *Remote Sensing of Environment*, Vol. 80, No. 3, pp. 460–472.

Elumnoh, A., and Shrestha, R.P. 2000. Application of DEM data to Landsat image classification: evaluation in a tropical wet–dry landscape of Thailand. *Photogrammetric Engineering & Remote Sensing*, Vol. 66, No. 3, pp. 297–304.

Franklin, J. 1991. Land cover stratification using Landsat Thematic Mapper data in Sahelian and Sudanian woodlands and wooded grassland. *Journal of Arid Environments*, Vol. 20, pp. 141–163.

Franklin, S., and Peddle, D. 1989. Spectral texture for improved class discrimination in complex terrain. *International Journal of Remote Sensing*, Vol. 10, No. 8, pp. 1437–1443.

Franklin, S., and Wulder, M. 2000. Remote sensing methods in medium spatial resolution satellite data land cover classification of large areas. *Progress in Physical Geography*, Vol. 26, No. 2, pp. 173–205.

Franklin, S., Connery, D., and Williams, J. 1994. Classification of alpine vegetation using Landsat thematic mapper, SPOT HRV, and DEM data. *Canadian Journal of Remote Sensing*, Vol. 20, No. 1, pp. 46–56.

Franklin, J., McCullogh, P., and Gray, C. 2000a. Terrain variables used for predictive mapping of vegetation communities in southern California. In *Terrain analysis: principles and applications.* Edited by J.P. Gallant and J.C. Wilson. John Wiley and Sons, Inc., New York. pp. 331–353.

Franklin, J., Woodcock, C.E., and Warbington, R. 2000b. Multi-attribute vegetation maps of Forest Service lands in California supporting resource management decisions. *Photogrammetric Engineering & Remote Sensing*, Vol. 66, No. 10, pp. 1209–1217.

Fuller, R., Groom, G., and Jones, A. 1994. The land cover map of Great Britain: an automated classification of Landsat Thematic Mapper data. *Photogrammetric Engineering & Remote Sensing*, Vol. 60, No. 5, pp. 553–562.

Giles, P.T. 2001. Remote sensing and cast shadows in mountainous terrain. *Photogrammetric Engineering & Remote Sensing*, Vol. 67, No. 7, pp. 833–839.

Hansen, M.C., DeFries, R.S., Townshend, J.R.G., and Sohlberg, R. 2000. Global land cover classification at 1 km spatial resolution using a classification tree approach. *International Journal of Remote Sensing*, Vol. 21, No. 6–7, pp. 1331–1364.

Homer, C., Ramsey, R., Edwards, T., Jr., and Falconer, A. 1997. Landscape cover-type modeling using a multi-scene thematic mapper mosaic. *Photogrammetric Engineering & Remote Sensing*, Vol. 63, No. 1, pp. 59–67.

Hutchinson, C. 1982. Techniques for combining Landsat and ancillary data for digital classification improvement. *Photogrammetric Engineering & Remote Sensing*, Vol. 48, No. 1, pp. 123–130.

Itten, K.I., and Meyer, P. 1993. Geometric and radiometric correction of TM data of mountainous forested areas. *IEEE Transactions on Geoscience and Remote Sensing*, Vol. 31, No. 4, pp. 764–770.

Kushwaha, S., Kuntz, S., and Oesten, G. 1994. Applications of image texture in forest classification. *International Journal of Remote Sensing*, Vol. 15, No. 11, pp. 2273–2284.

Leprieur, C., Durrand, J., and Peyron, J. 1988. Influence of topography on forest reflectance using Landsat Thematic Mapper and digital terrain data. *Photogrammetric Engineering & Remote Sensing*, Vol. 54, No. 4, pp. 491–496.

Lillesand, T.M., and Kiefer, R.W. 1987. *Remote sensing and image interpretation*. 2nd ed. John Wiley & Sons Inc., New York.

Loveland, T.R., and Belward, A.S. 1997. The IGBP-DIS global 1-km land cover data set, DISCover: first results. *International Journal of Remote Sensing*, Vol. 18, No. 15, pp. 3289–3295.

Loveland, T.R., Merchant, J., Ohlen, D., and Brown, J. 1991. Development of land-cover characteristics database for the conterminous United States. *Photogrammetric Engineering & Remote Sensing*, Vol. 57, No. 11, pp. 1453–1463.

Loveland, T.R., Reed, B.C., Brown, J.F., Ohlen, D.O., Zhu, Z., Yang, L., and Merchant, J.W. 2000. Development of a global land cover characteristic database and IGBP DISCover from 1 km AVHRR data. *International Journal of Remote Sensing*, Vol. 21, No. 6–7, pp. 1303–1330.

Markham, B., and Barker, J. 1986. Landsat MSS and TM post calibration dynamic ranges, exoatmospheric reflectances and at satellite temperature. *EOSAT Landsat Technical Notes*, Vol. 1, pp. 3–7.

McGuffie, K., and Henderson-Sellers, A. 1986. Illustration of the influence of shadowing on high latitude information derived from satellite imagery. *International Journal of Remote Sensing*, Vol. 7, No. 10, pp. 1359–1365.

Meyer, P., Itten, K., Kellenberger, T., Sandmeier, S., and Sandmeier, R. 1993. Radiometric corrections of topographically induced effects on Landsat TM data in an alpine environment. *ISPRS Journal of Photogrammetry and Remote Sensing*, Vol. 48, No. 4, pp. 17–28.

Peddle, D., Teillet, P.M., and Wulder, M. 2003. Radiometric image processing. In *Remote sensing of forest environments: concepts and case studies*. Edited by M. Wulder and S. Franklin. Kluwer Academic Publishers, Dordrecht, The Netherlands. pp. 181–208.

Sader, S.A., Waide, R.B., Lawrence, W.T., and Joyce, A.T. 1989. Tropical forest biomass and successional age class relationships to a vegetation index derived from Landsat TM data. *Remote Sensing of Environment*, Vol. 28, No. 1, pp. 143–156.

Skidmore, A. 1989. An expert system classifies eucalypt forest types using Thematic Mapper data and a digital terrain model. *Photogrammetric Engineering & Remote Sensing*, Vol. 55, No. 10, pp. 1449–1464.

Stone, T., Schlesinger, P., Houghton, T., and Woodwell, G. 1994. A map of the vegetation of South America based on satellite imagery. *Photogrammetric Engineering & Remote Sensing*, Vol. 60, No. 5, pp. 541–551.

Strahler, A. 1981. Stratification of natural vegetation for forest and rangeland inventory using Landsat digital imagery and collateral data. *International Journal of Remote Sensing*, Vol. 2, No. 1, pp. 15–41.

Strahler, A., Logan, T., and Bryant, N. 1978. Improving forest cover classification accuracy from Landsat by incorporating topographic information. In *Proceedings of the 12th International Symposium on Remote Sensing of the Environment*, Manila, Philippines. Environmental Research Institute of Michigan (ERIM), Ann Arbor, Mich. pp. 927–942.

Swain, P.H., and Davis, S.M. (Editors). 1978. *Remote sensing: the quantitative approach*. McGraw-Hill, Inc., New York.

Teillet, P.M., Guindon, B., and Goodenough, D.G. 1982. On the slope-aspect correction of multispectral scanner data. *Canadian Journal of Remote Sensing*, Vol. 8, No. 2, pp. 84–106.

Tou, J.T., and Gonzalez, R.C. 1974. *Pattern recognition principles*. Addison-Wesley Publishing Co., Reading, Mass.

Wulder, M., and Nelson, T. 2001. *EOSD land cover classification legend report, version 1*. Pacific Forestry Centre, Canadian Forest Service, Natural Resources Canada, Victoria, B.C. 89 pp.

Wulder, M., and Seemann, D. 2001. Spatially partitioning Canada with the Landsat Worldwide Referencing System. *Canadian Journal of Remote Sensing*, Vol. 27, No. 3, pp. 225–231.

Wulder, M., Cranny, M., and Dechka, J. 2002. *An illustrated methodology for land cover mapping of forests with Landsat-7 ETM+ data: methods in support of EOSD land cover, version 2*. Pacific Forestry Centre, Canadian Forest Service, Natural Resources Canada, Victoria, B.C. 39 pp.

Wulder, M.A., Dechka, J.A., Gillis, M.A., Luther, J.E., Hall, R.J., Beaudoin, A., and Franklin, S.E. 2003. Operational mapping of the land cover of the forested area of Canada with Landsat data: EOSD land cover program. *Forestry Chronicle*, Vol. 79, No. 6, pp. 1075–1083.